JOURNAL OF APPLIED ELECTROCHEMISTRY 19 (1989) 657–667

The vertical distribution of current in a gas-evolving membrane cell*

A. D. MARTIN‡, A. A. WRAGG

Chemical Engineering Department, University of Exeter, Exeter EX4 4QF, UK

Received 8 July 1988; revised 4 January 1989

A one-dimensional numerical model to describe gas void fraction and current distribution in five model membrane cell configurations is described in this work. The five models describe ideal (equipotential), upright (top cathode/bottom anode), inverted, u- and n-type electrical connections with anodic chlorine and cathodic hydrogen evolution in each case. In all but the first case the finite resistances of the electrodes are taken into account. The effects of (a) different terminal arrangements, (b) different current densities, (c) different cell heights, (d) different compartment widths, and (e) different overvoltages, have been investigated. For each study the current distribution and anolyte and catholyte void fraction distribution is displayed. The resistive components of the cell voltages are also calculated; the calculated resistive voltage loss varies between extremes of 0.291 V for the ideal cell to 0.377 V for the inverted cell at 3 kA m^{-2} and 0.25 m cell height with typical fixed values of other parameters.

Nomenclature

A	cross-sectional area
d	bubble diameter
ε	void fraction
ε_m	maximum void fraction
G	gas volumetric flow rate
K	ratio of conductivities of bubble-free and bubble-filled electrolyte
L	liquid volumetric flow rate
μ	electrolyte viscosity
R_{AN}, R_A, R_M, R_C, R_{CA}	resistances of anode, anolyte, membrane, cathode and catholyte, respectively (see resistive network scheme of Fig. 2)
ϱ_L, ϱ_G	liquid and gas phase densities
u_1	single bubble rise velocity
u_{sw}	bubble swarm rise velocity

1. Introduction

The advent of compact, high current density electrolysers has prompted considerable research effort towards the prediction of cell voltages and potential and current distribution for cells with complex geometry and/or with gas evolution. Such information is necessary to the choice of operating current density, electrode spacing and cell connection arrangements, and knowledge of current distribution is also important to the life of membranes and catalyst coatings.

A series of papers by Nishiki *et al.* [1–6] has dealt with a number of model electrode geometries in gas-evolving cells using the finite element modelling method. Our group has also carried out work on model chlor–alkali membrane cells with variation of electrode blade geometry, membrane–electrode spacing, membrane contortion and overpotential [7, 8]. The finite difference method employed for use with the complex shapes involved was introduced in [8] along with limited results for electrode and membrane current distributions for eight different electrode blade shapes. Further results from this study will be published later [9].

Other notable recent contributions in this area are those described by Tobias and co-workers, e.g. [10, 11], the latter involving the modelling of the effect of attached bubbles on potential drop and current distribution at gas-evolving electrodes. Also, Divisek [12] has considered current distribution–electrode potential relations for a bipolar water electrolysis cell and Bisang and Kreysa [13] have recently considered the effect of electrode resistance on current density distribution in a cylindrical reactor both experimentally and mathematically.

The present modelling exercise departs from the assumption of uniform gas voidage [8], and hence uniform electrolyte resistivity through the cell, to consider the case where electrolyte resistivity varies considerably in the vertical direction. In particular the effects of varying cell connection arrangements are investigated.

It is well known that in a gas-evolving cell the void fraction and, therefore, the electrolyte resistivities,

* Paper presented at the 2nd International Symposium on Electrolytic Bubbles organized jointly by the Electrochemical Technology Group of the Society of Chemical Industry and the Electrochemistry Group of the Royal Society of Chemistry and held at Imperial College, London, 31st May and 1st June 1988.

‡ *Present address*: ICI, Chemicals and Polymers Ltd, Castner-Kellner Works, P.O. Box 9, Runcorn, Cheshire WA7 4JE, UK.

0021-891X/89 $03.00 + .12

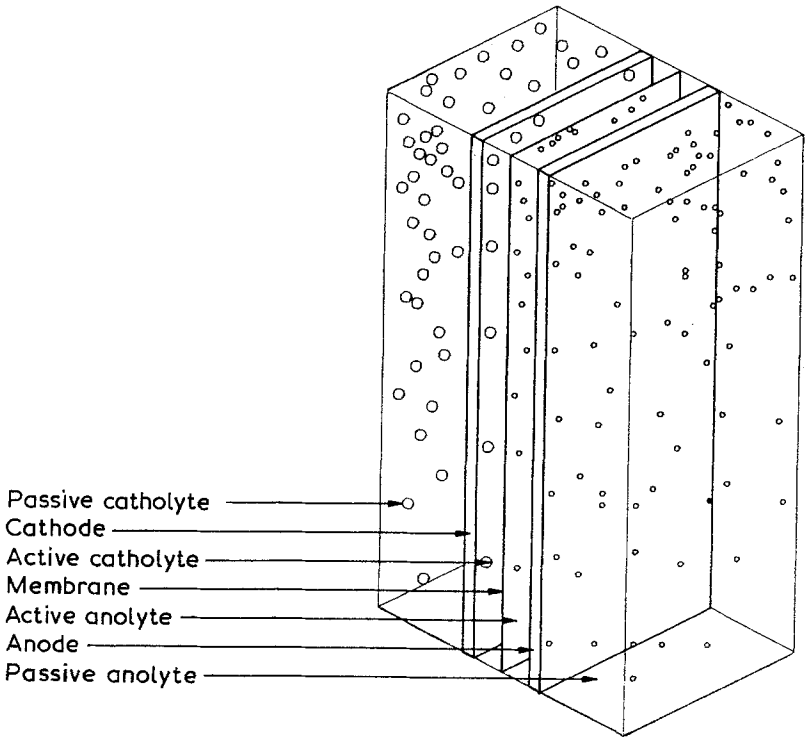

Fig. 1. Depiction of model gas-evolving membrane cell.

increase with distance up the cell. The resistivity of a gas-filled electrolyte may change by a factor of four between the bottom and top of the cell and this can have a profound effect on the distribution of current. A simple one-dimensional model of the vertical section has been developed with electrodes of finite cross-section and conductivity (Fig. 1). The electrolytes are divided into two volumes: the active electrolyte situated between the electrodes and the passive electrolyte situated behind the electrodes. The passive electrolyte serves as a reservoir of reagents and a channel through which the evolved bubbles rise to the surface of the electrolyte. The electrodes are of the pressed 'lantern' type as described elsewhere [7].

2. Model basis

The model has been developed in the light of previous work by Tobias [14], Funk and Thorpe [15] and Nagy [16] and the results of experimental work carried out on operational chlor-alkali membrane cells [7]. The three models mentioned above consider broadly similar geometries, i.e. a tall, narrow channel with equipotential electrodes. All the above models contain assumptions which limit their use to low void fraction systems and also assume that the upper limit on the void fraction is 1.0. Most of the assumptions made are attempts to linearize a strongly non-linear problem. Any model which seeks to reproduce the behaviour of an operational commercial cell must be free from the assumptions that lead to these constraints.

The model developed here is based on the Kreysa and Kuhn [17] coalescence barrier model.

$$u_{sw}\frac{\varepsilon}{\varepsilon_m} = \frac{G}{\varepsilon A} - \frac{G}{\varepsilon_m A} - \frac{L}{\varepsilon_m A}\left(\frac{\varepsilon_m - \varepsilon}{1 - \varepsilon}\right) \quad (1)$$

This model, represented by Equation 1, when combined with relationships describing the motion of the bubbles such as the Marrucci [18] expression (Equation 2)

$$u_{sw} = u_1 \frac{(1 - \varepsilon)^2}{(1 - \varepsilon^{5/3})} \quad (2)$$

yields a relationship describing the behaviour of the bubble swarm which is not only non-linear but also implicit. Here the single bubble rise velocity, u_1, is calculated from the Levich equation [19]

$$u_1 = \frac{d^2 g}{12\mu}(\varrho_L - \varrho_G) \quad (3)$$

The combined coalescence barrier model provides a relationship between the gas and liquid superficial velocities and the void fraction of the electrolyte. Further expressions to describe the resistivity of the electrolyte in terms of its void fraction and the overvoltage in terms of the local current density are added. To describe the electrolyte resistivity the Prager [20] expression is used.

$$K = 1 - \frac{\varepsilon}{2} + \frac{\varepsilon^2}{2} \quad (4)$$

This expression was developed to take into consideration particle interactions in concentrated suspensions and is, consequently, applicable over a wide range of void fractions. A simple Tafel-type overvoltage relationship is used to describe the electrode kinetics.

A number of important assumptions have to be made in the process of discretization: (1) the current flows unidirectionally; this assumption is implicit in the one-dimensional model; (2) the bubble size distribution can be adequately described by a single mean throughout any one horizontal section; (3) detaching bubbles reach their terminal velocities instantaneously.

The assumptions have effects of different orders of magnitude. The first, and perhaps the most fundamental, assumption arises directly from the consideration of a one-dimensional model. This assumption is

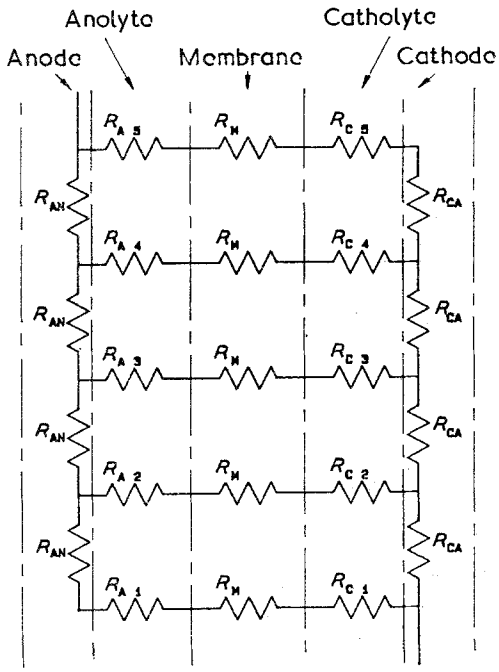

Fig. 2. Resistive network analogue for the inverted vertical membrane cell model.

more valid at low interelectrode gaps and low overvoltage gradients with respect to current density, i.e. high membrane relative resistivity, high current densities, low volumetric gas production and low Tafel coefficients.

Assumption (2) is quite loose. This condition is only allowable because the derivations used by Prager [20], in the development of his expression for the diffusivity in an arbitrary suspension, are also very general. This assumption has important corollaries, the first being that the bubbles can be considered to rise *en masse* to the next discrete level in the model, i.e. a single bubble rise velocity can be used to describe the motion of the whole swarm, and the second is that no implicit assumption is made about the form of the bubble size distribution.

The third assumption is expected to have little influence on the results obtained since the bubbles are of very low mass. It can be easily proved that a typical bubble in this system reaches 99% of its terminal velocity in approximately 3 ms, during which time the bubble has moved less than one diameter.

The assumption of a uniform bubble diameter has been checked and found to have very little effect on the results of a number of test cases including a series of very tall (1.5 m) cells. In a 1.5-m-tall cell it can be calculated that the bubble diameter will increase by 5% due to the static pressure difference between the bottom and the top of the electrolyte, causing a 10% increase in bubble rise velocity.

The assumption of a linear overvoltage relationship made by Tobias [14] has been checked and found to be valid over the relevant range of current densities. However it was felt necessary to retain this assumption in this piece of work.

It is further assumed that the cell is isothermal in operation. This assumption can be justified in that under normal operating conditions the bubble effects dominate the effects of even quite large temperature gradients.

2.1. *Discretization*

A simple discretization scheme has been used to produce a resistive network analogue of the processes involved (Fig. 2). The resistive network analogue method is described in some detail by Wardle [21] for a very much simpler model of the electrolyte.

The coalescence barrier model as proposed by Kreysa and Kuhn [17] leads to a finite difference analogue containing nested iterative loops. The shell loop consists of the steps required to solve the set of equations resulting from the resistive network analysis. The kernel loops comprise the steps required to solve the coalescence barrier model, calculate the electrolyte resistivities and the Tafel overvoltage. Thus, much of the discretization involved the development of computing techniques to yield rapid solutions from the kernel loops. Fortunately the coalescence barrier model is amenable to the direct substitution method. This means that as the calculation proceeds

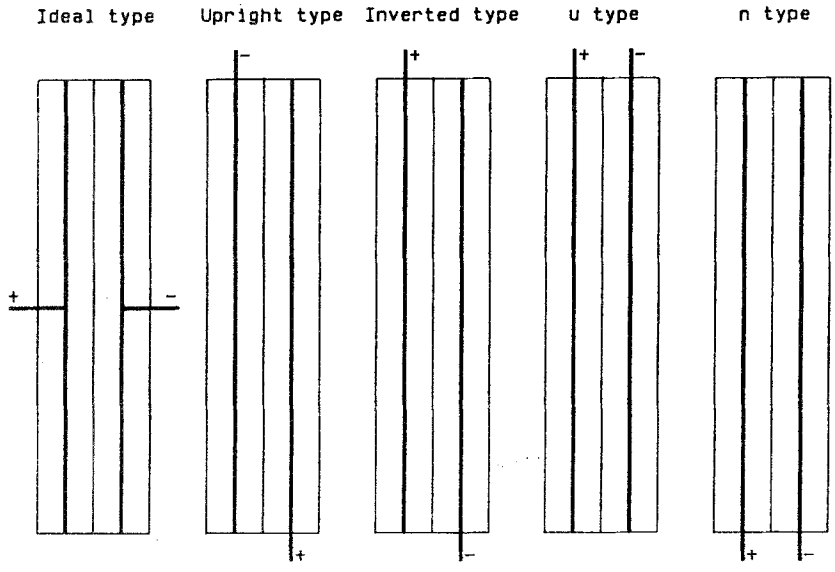

Fig. 3. Model cell configurations.

Table 1. Values of fixed parameters used in modelling

Electrode pitch	7 mm	Anolyte viscosity	1.0×10^{-3} kg m^{-1} s^{-1}
Cell height	250 mm	Catholyte viscosity	6.0×10^{-3} kg m^{-1} s^{-1}
Electrode lantern widths	8.8 mm	Anolyte density	1.15×10^{3} kg m^{-3}
Electrode blade thicknesses	1.2 mm	Catholyte density	1.34×10^{3} kg m^{-3}
Electrode-to-membrane gaps	1 mm	Max anolyte void fraction	0.642
Membrane thickness	0.24 mm	Max catholyte void fraction	0.252
Anode resistivity	7.5×10^{-7} Ω m	Chlorine bubble size[1]	0.295 mm
Cathode resistivity	1.4×10^{-7} Ω m	Hydrogen bubble size[1]	1.40 mm
Anolyte resistivity	1.2×10^{-2} Ω m	Temperature	85° C
Catholyte resistivity	8.0×10^{-3} Ω m	Pressure	101.5 kPa
Membrane resistivity	3.3×10^{-1} Ω m	Current density[2]	3 kA m^{-2}
Anolyte concentration	1.9×10^{-1} kg kg^{-1}	kmole gas per Faraday	5×10^{-4}
Catholyte concentration	3.2×10^{-1} kg kg^{-1}	Liquid superficial velocity	0 m s^{-1}

[1] 0.325 and 1.5 mm, respectively in cell height study.
[2] 2 kA m^{-2} in cell height study.

the kernel iterations are progressively compressed and eventually eliminated, hence considerably improving the speed of successive passes through the main shell iteration. Obtaining convergence in the kernel loops has been found to be vital to the stability of the shell calculations, particularly in the early stages of the shell iteration. This implies that it is not possible to dispense with the kernel loops.

Versions of the model have been developed to investigate the 'ideal' cell with equipotential electrodes, and a number of 'real' cells containing electrodes of finite resistivity and having terminals in various positions (Fig. 3). These cells have been termed the 'ideal' type (equipotential electrodes), the 'upright' and 'inverted' (according to the position of the low resistance electrode contact at the top or bottom of the cell respectively), the 'n'-type (both electrode contacts situated at the bottom) and the 'u'-type (both electrode terminals at the top of the cell). Some of these configurations are impractical as operational cells but serve to show the effects of a restricted number of contacts in a practical design of that particular type.

3. Results and discussion

As a result of a validation study [7] it was decided to set the bubble diameters and limiting void fractions to 0.295 mm and 0.642 for the anolyte and 1.40 mm and 0.252 for the catholyte. Holding other parameters at the values indicated in Table 1, the effects of the following were investigated: (1) differing cell configurations (see Fig. 3); (2) differing current densities; (3) differing cell heights; (4) differing compartment widths; (5) differing overpotential effects. The values of the floating parameters were varied as indicated in Table 2.

Table 2. Floating parameters were varied as follows

Current density	2.0, 2.5, 3.0, 3.5, 4.0 kA m^{-2}
Cell height	0.25, 0.5, 0.75, 1.0, 1.25 m
Electrode lantern width	2, 4, 6, 8, 10 mm
Tafel coefficient	0, 0.125, 0.250, 0.50, 1.00 V

3.1. *Cell configuration effects*

The configuration of the cell influences the distribution of current density quite dramatically (Fig. 4) as the electrolytes are of non-uniform resistivity and the electrode resistances differ markedly. Thus, judicious arrangement of the components of a cell can help to eliminate non-uniformities caused by the gas-filled electrolytes without excess sacrifice to resistive losses. The 'u'- and 'n'-types of cell show particularly poor distribution of current, especially the 'n'-type which combines the shortest electrical path with the lowest resistance electrolytes. This results in a large current density at the bottom of the cell. The 'upright' and 'inverted' cells show that a simple change of electrode connection can improve the distribution of current significantly. Clearly the current distribution can be further modified by changing the electrode cross-sectional areas to yield a combination that virtually eliminates the effects of the electrolyte void fractions. The 'ideal' cell shows the effect of the gas-filled electrolyte in isolation. Unfortunately the non-linearity of the problem prevents the subtraction of this result from the others to yield the electrode resistance effect in isolation.

The void fractions (Fig. 5) exhibit remarkably small differences, reinforcing the suggestion that the potential distribution calculation can be decoupled from the void fraction calculation without introducing excessive errors. This is particularly true of the catholyte void fraction distributions which do not exhibit a limiting void fraction or a choked electrolyte [7].

Table 3 shows the predicted resistive voltage losses for the different cell configurations at 3.0 kA m^{-2}.

Table 3. Resistive voltage losses for the five cell configurations

Cell type	*Resistive voltage loss at 3.0 kA m^{-2} (V)*
Ideal type	0.291
Upright type	0.374
Inverted type	0.377
n-type	0.371
u-type	0.267

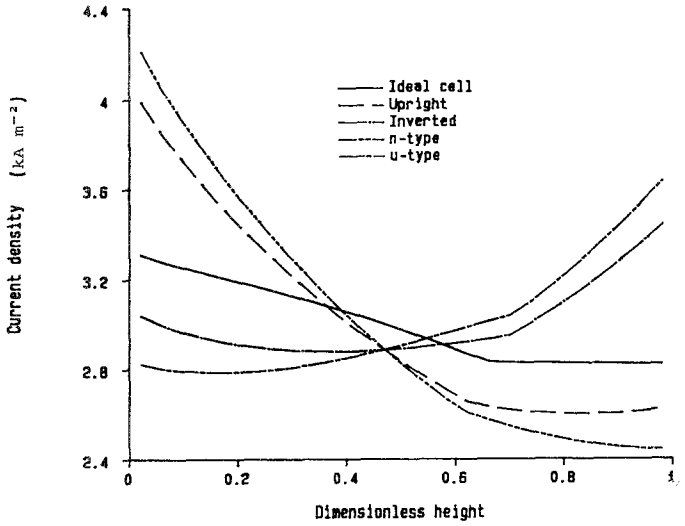

Fig. 4. Current distributions in cells of various configuration.

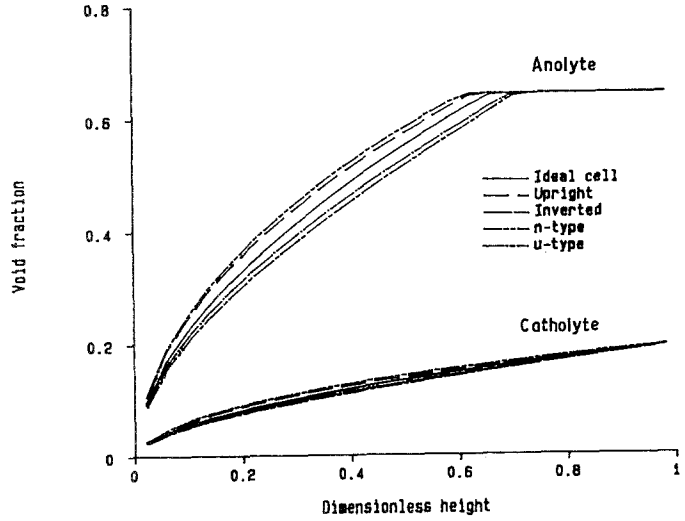

Fig. 5. Void fraction distributions in cells of various configuration corresponding to the current distribution curves of Fig. 4.

The 'ideal' and 'u'-type cells exhibit the two lowest resistive losses. The 'ideal' cell has an advantage over the 'u'-type as the electrode resistivities make no contribution to the voltage loss. Despite the disadvantage caused by finite electrode conductivities the 'u'-type cell exhibits the lower resistive voltage loss. This is due to a substantial part of the current passing through the top of the cell from which the gas can easily escape thus lowering the overall resistance of the electrolytes. Figure 5 shows that the 'u'-type cell exhibits the lowest void fraction throughout the unchoked regions. The three remaining cell types show very similar resistive voltage losses whilst also showing considerably different current distributions. These results highlight what can be done in terms of optimization of the cell configuration with little sacrifice to further resistive losses.

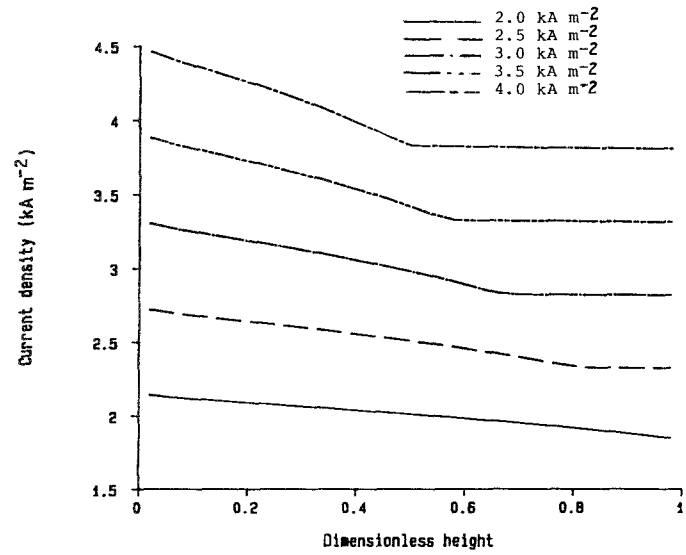

Fig. 6. Effect of mean operating current density on current distribution in 'ideal' cells.

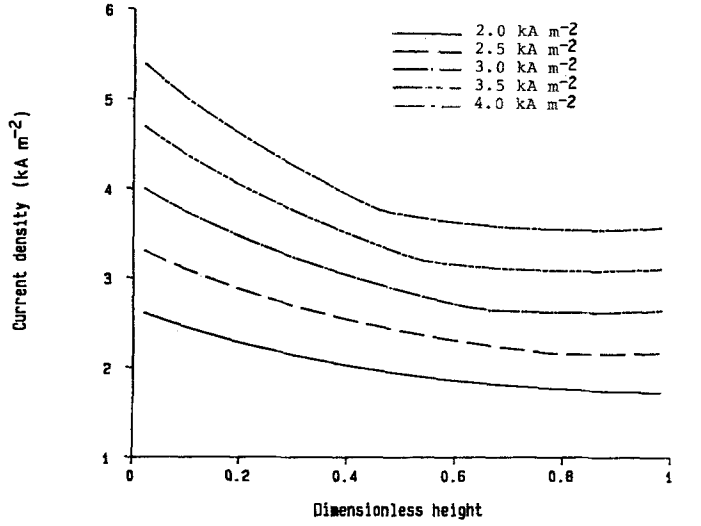

Fig. 7. Effect of mean operating current density on current distribution in 'upright' cells.

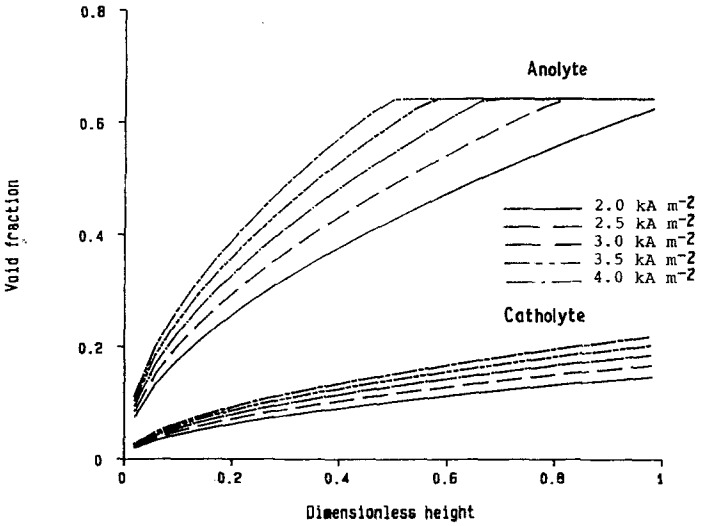

Fig. 8. Effect of mean operating current density on void fraction in 'ideal' cells.

3.2. *Mean current density effects*

This part of the study aimed to explore the effects of a range of normal operating mean current densities on the 'ideal' and the 'upright' cell types. At low mean current densities both cells exhibit smoothly descending current distribution curves (Figs 6 and 7). The smooth descent is due to the lack of a void fraction limited region. The current distribution in the 'ideal' cell (Fig. 6) shows a small region of positive curvature at the foot followed by a region of negative curvature that occupies a substantial portion of the unchoked cell; this zone is joined to the uniform part of the current distribution by a region of very high positive curvature. This is in sharp contrast to the results presented by Tobias [14], Funk and Thorpe [15] and Nagy [16], all of whom found the local current density to vary monotonically throughout the cell. The current distribution in the 'upright' cell type shows a wider variation of local current density than the ideal cell. The

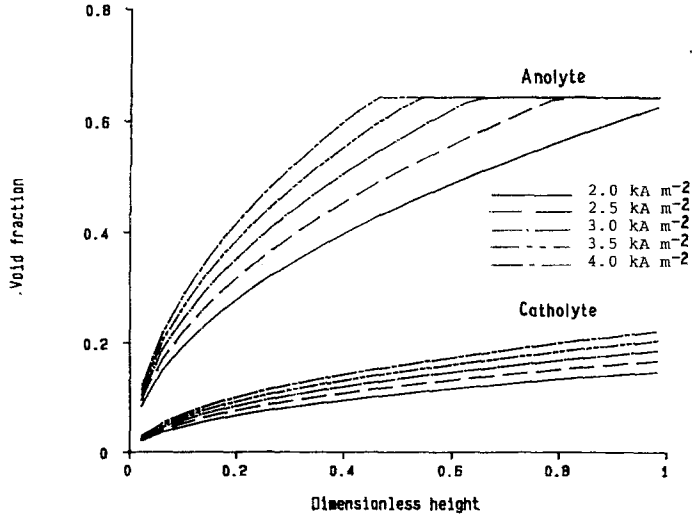

Fig. 9. Effect of mean operating current density on void fraction distribution in 'upright' cells.

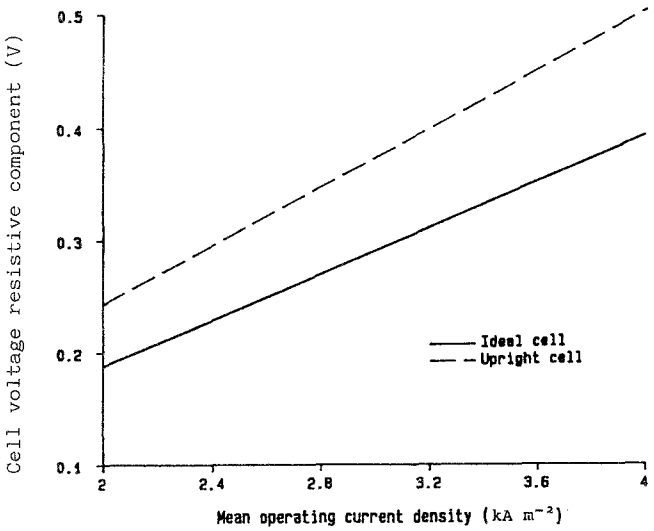

Fig. 10. Effect of operating current density on resistive component of cell voltage.

curves corresponding to cells with a choked region at the top also show a minimum current density in that area. The position of the minimum is found to be independent of the mean current density and to occur at approximately 82% of the height of the cell.

The void fraction profiles show broadly similar behaviour (Figs 8 and 9). The catholytes do not exhibit any limiting behaviour which is consistent with the findings of the experimental work reported in [7]. The anolyte void fraction profiles in the 'upright' cell show a more rapid approach to the limiting value than in the 'ideal' cell. This is easily accounted for by the biasing of the current distribution toward the lower part of the cell, which is caused by the differing electrode resistances.

The relationship between the operating current density and the cell resistive voltage losses is almost linear for both the 'ideal' and 'upright' cells (Fig. 10). However the upright cell shows a slight upward curvature suggesting that this cell type is more sensitive to the redistribution of void fraction than the 'ideal' cell. The expansion of the choked electrolyte region down the

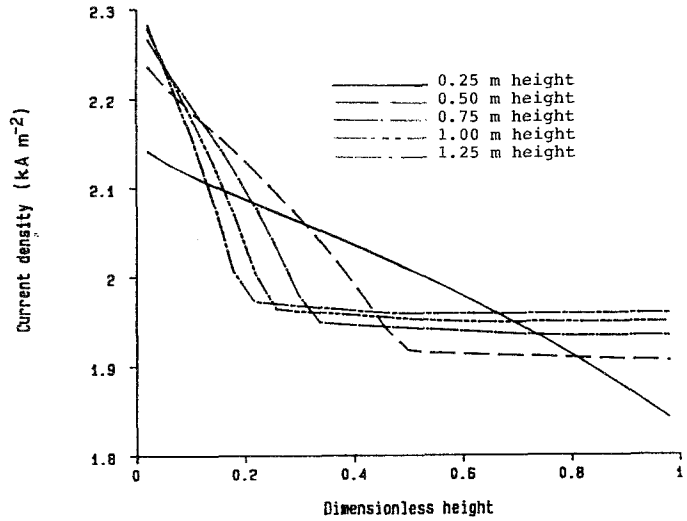

Fig. 11. Current distribution in 'ideal' cells of various heights.

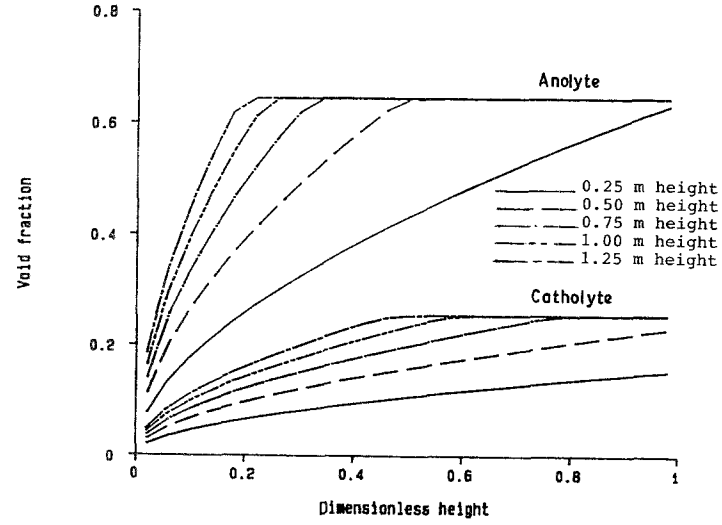

Fig. 12. Void fraction distributions in 'ideal' cells of various heights.

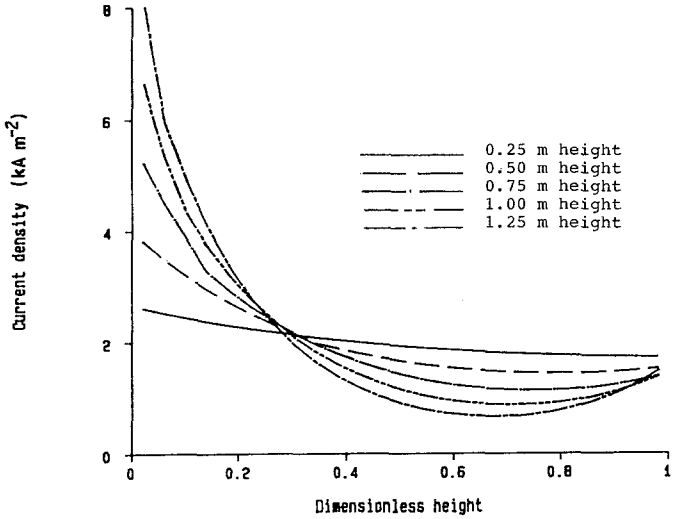

Fig. 13. Current distributions in 'upright' cells of various heights.

cell causes a general increase in the cell resistance; added to this is the effect of a changed proportion of the electrical path lying in the higher resistance anode.

3.3. *Cell height effects*

The 'ideal' cell shows a relatively uniform distribution of current (Fig. 11). This is partly due to the very narrow electrolyte gaps of 1.0 mm, but most significantly to the assumption of ideal equipotential electrodes. The distribution of current throughout the choked portion of the cell is very uniform. This is to be expected as the interelectrode resistance is also constant.

The void fraction distributions (Fig. 12) show that the position of the onset of choked behaviour is independent of the total height and occurs at about 260 mm above the foot of the cell.

The distribution of current in the 'upright cell' (Fig. 13) is much less uniform than that in the 'ideal' cell. This reflects the importance of the electrode resistances on the distribution of current. Optimization of the electrode design could use this effect to advantage and help to eliminate the variations shown by the 'ideal' cell. As the height of the cells is increased the electrode effect grows considerably leading to very poor current distribution in the 1.25-m-tall cell. This gross maldistribution of current has profound effects on the distribution of void fraction (Fig. 14). The choked region can be seen to almost completely fill the cell when the height has reached 1.25 m. This further increases the cell resistance. All the cases that exhibit a choked electrolyte also show a minimum in the current distribution. This minimum becomes stronger as the cell is made progressively taller; it is also found to move down the cell. In the 1.25-m-tall case the maximum current density is four times the desired mean operating current density.

Figure 12 shows clearly how the poor distribution of current has affected the distribution of void fraction. Unlike the 'ideal' cell the position of the onset of choked behaviour is quite strongly dependent on cell height. The location of the bottom of the choked region moves rapidly down the cell as the height is increased until in the 1.25-m-tall case this region occupies 96% of the channel volume. The results from the 'upright' cell type suggest that, in tall cells, it is not possible to decouple the current distribution and void fraction calculations, since the gross maldistribution of current clearly has a profound effect on the distribution of void fraction. However the results from the 'ideal' cell suggest the reverse is still true for that type of design.

As the height of the cell is increased the rate of

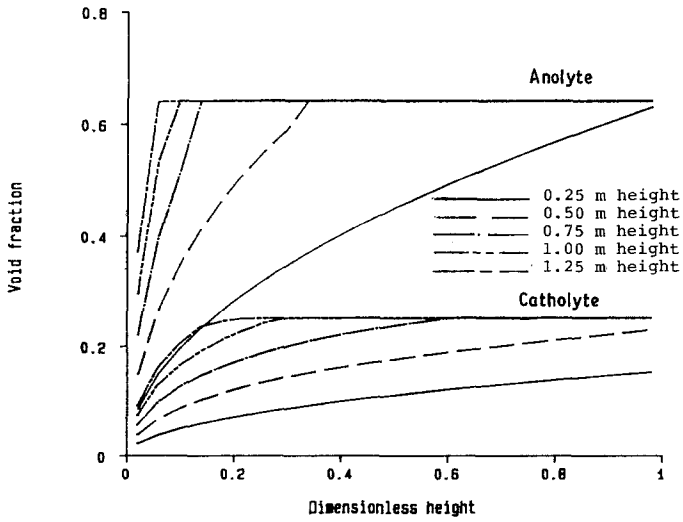

Fig. 14. Void fraction distributions in 'upright' cells of various heights.

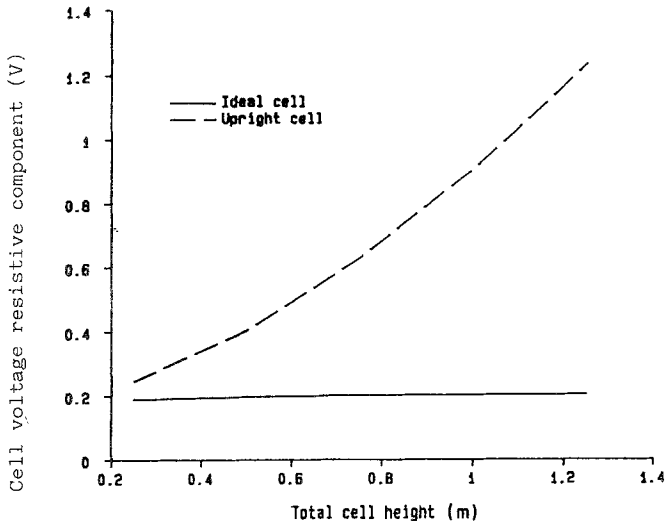

Fig. 15. Effect of total cell height on resistive component of cell voltage.

increase of resistive voltage losses exhibited by the 'upright' cell grows (Fig. 15). This is due to the combination of longer electrodes with a greater proportion of the anolyte being choked with bubbles. The 'ideal' cell shows resistive losses that are almost independent of the height of the cell. This results from the narrow interelectrode gap and the high resistivity of the membrane.

3.4. *'Lantern' and compartment width effects*

The electrode lantern width, as described in [8], governs the amount of floor area required for a given plant capacity. Thus its minimization is highly desirable. In this section of the study the electrode-to-membrane gaps were maintained constant. Hence variation of the lantern width directly affects the width of the compartment. The results show the effects of reducing the area available for the escape of evolved gas. Selected results only are shown here, further detail and fuller discussion being available elsewhere [7]. It can be seen in Fig. 16 that for the 'upright' cell the maximum current density at the foot of the cell is remarkably unaffected by the compartment width (the distance between the membrane and the back of the electrolyte channel) and the commensurate redistribution of void fraction. All the current distributions show a minimum in the choked region. The minimum is independent of the compartment width and occurs at 82% of the cell height.

As the width of the compartment is reduced the resistive losses shown by both the 'ideal' and 'upright' cells increase slightly (Fig. 17). The relationship is virtually linear in both cases; however, the 'upright' cell does show a small positive curvature. The low dependence on compartment width is due to the narrow interelectrode gap. If the compartment width had been adjusted by manipulating the electrode to membrane gaps a very much stronger dependence would have been expected.

3.5. *Overvoltage effects*

The effect of overvoltage on the distribution of current in electrolytic cells is well documented. The current distribution becomes more uniform the higher the gradient of the overvoltage relationship. The levelling effect of the Tafel gradient on the current distribution becomes less significant the higher the current density. Closer examination of the Tafel relationship suggests that the absolute value of current density is unimportant and it is the relative values of the maximum and

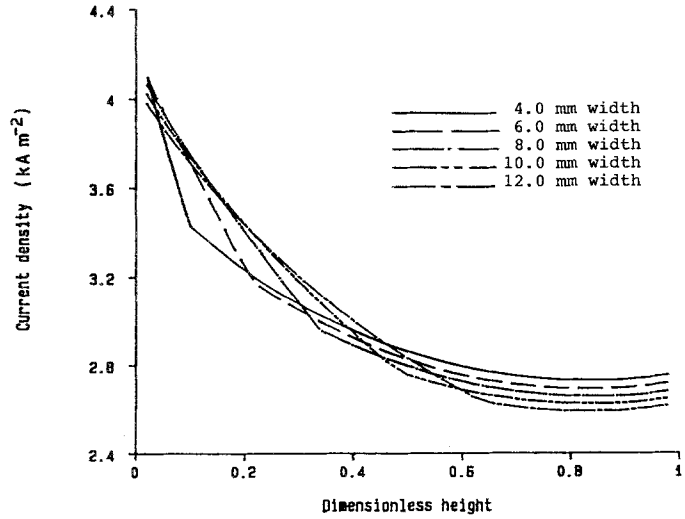

Fig. 16. Effect of compartment width on current distribution in 'upright' cells.

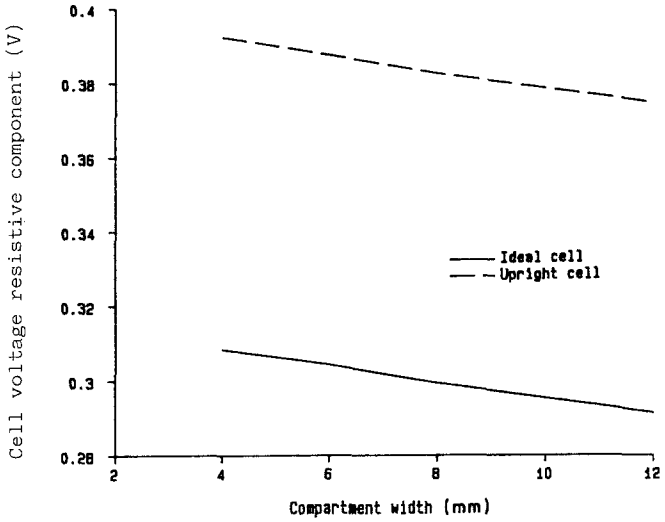

Fig. 17. Effect of compartment width on resistive component of cell voltage.

minimum current density which determine the degree of levelling. Thus it is possible to assign an arbitrary, but convenient, value to the exchange current density term that yields a useful zero in the overvoltage relationship. In this work the exchange current density has been set to 1.0 A m^{-2}. Details of the remaining cell parameters can be found in Table 1. Figure 18 clearly shows the levelling effect of overvoltage which occurs particularly in the case of the 'upright' cell in which the current distribution is initially much less uniform. The 'upright' cell also shows a weak minimum in the current distributions at the 82% level. The minimum becomes weaker with increasing Tafel coefficient, which is to be expected from the normal levelling effect of overvoltage. In both the 'ideal' and 'upright' cases all the current distributions cross at the same position; at the 46% level and 3.01 kA m^{-2} in the case of the 'ideal' cell and at the 40% level and 3.00 kA m^{-2} in the 'upright' cell.

Other results, especially for the effect of Tafel coefficient on void fraction distribution and on the resistive component of the cell voltage, are again given elsewhere [7]. Both 'ideal' and 'upright' cell types show a perfectly linear relationship between the cell voltage and Tafel coefficient in the range investigated. This result is not unexpected in view of the narrow inter-electrode gap and the minimal effect overvoltage has on the distribution of void fraction.

4. Conclusions

Among the conclusions from this numerical modelling exercise the following may be highlighted.

(i) The distribution of void fraction has been shown to be remarkably resistant to changes in the pattern of current distribution and, therefore, gas evolution distribution.

(ii) It has been found that only under certain specialized conditions is it possible to calculate the void fraction profile independently of the current distribution.

(iii) Despite the relatively high conductivities of the electrodes relative to those of the electrolytes, electrode conductivity has been shown to have a profound effect on the vertical distribution of current and to produce a minimum current density in the 'upright' and 'inverted' configurations.

(iv) The location of the minimum current density exhibited by the 'upright' configuration has been found to be independent of compartment width and Tafel gradient, thus confirming this minimum to be an electrode length and conductivity effect.

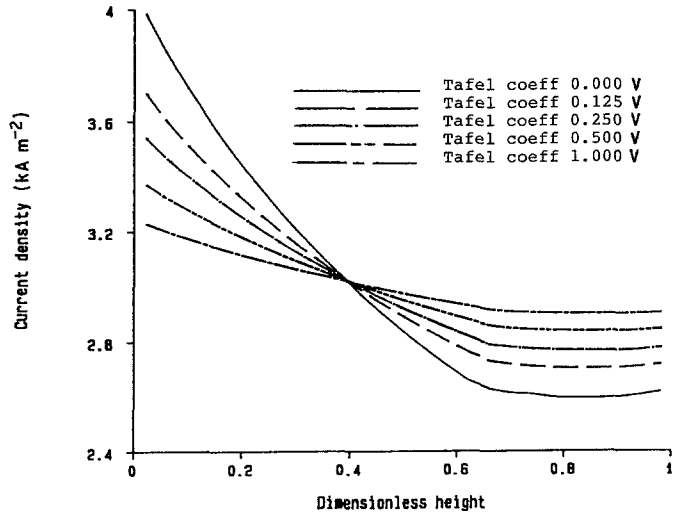

Fig. 18. Effect of overvoltage on current distribution in 'upright' cells.

(v) The study of cell configuration indicates clearly that it is possible to optimize the distribution of current by careful selection of the configuration having regard for electrode thicknesses and conductivities.

(vi) The study examining the effects of Tafel gradient shows clearly that even very high values of the gradient are insufficient to promote a uniform current distribution in either the 'ideal' cell or the 'upright' configuration. From this study it can also be concluded that the void fraction profile is virtually independent of the assumed electrode kinetics.

(vii) The study of the effects of cell height shows that it is advantageous in both 'ideal' and 'upright' configurations to design a short (low) cell in order to achieve the most uniform distribution of current.

Acknowledgement

The authors wish to acknowledge support of this work by the Science and Engineering Research Council and ICI plc.

References

[1] Y. Nishiki, K. Aoki, K. Tokuda and H. Matsuda, *J. Appl. Electrochem.* **14** (1984) 653.
[2] *Idem, ibid.* **16** (1986) 291.
[3] *Idem, ibid.* **16** (1986) 615.
[4] *Idem, ibid.* **17** (1987) 67.
[5] *Idem, ibid.* **17** (1987) 445.
[6] *Idem, ibid.* **17** (1987) 552.
[7] A. D. Martin, The influence of void fraction and geometry on current distribution in chlor–alkali membrane cells. PhD Thesis, University of Exeter (1985).
[8] A. D. Martin, A. A. Wragg and J. C. R. Turner, Inst. Chem. Engrs Symp. Series 98, Electrochemical Engineering, Loughborough (1986) p. 35.
[9] A. D. Martin, A. A. Wragg and J. C. R. Turner, to be published.
[10] G. A. Prentice and C. W. Tobias, *J. Electrochem. Soc.* **129** (1982) 72.
[11] J. Dukovic and C. W. Tobias, *J. Electrochem. Soc.* **134** (1987) 331.
[12] J. Divisek, *J. Appl. Electrochem.* **14** (1984) 663.
[13] J. M. Bisang and G. Kreysa, *J. Appl. Electrochem.* **18** (1988) 422.
[14] C. W. Tobias, *J. Electrochem. Soc.* **106** (1959) 833.
[15] J. E. Funk and J. F. Thorpe, *J. Electrochem. Soc.* **116** (1969) 48.
[16] Z. Nagy, *J. Appl. Electrochem.* **6** (1976) 171.
[17] G. Kreysa and M. Kuhn, *J. Appl. Electrochem.* **15** (1985) 517.
[18] G. Marrucci, *Ind. Eng. Chem. Fundam.* **42** (1965) 224.
[19] V. G. Levich, 'Physicochemical Hydrodynamics', Prentice-Hall, NJ (1962) pp. 434–448.
[20] S. Prager, *Physica* **29** (1963) 129.
[21] I. Wardle, paper read at A.I.Ch.E. Spring National Meeting, Houston, Texas, March (1983).